Peer-reviewed version available at *Appl. Sci.* **2020**, *10*, 3597; doi:10.3390/app10103597

Article

Study on the Vibration Isolation Performance of Composite Subgrade Structure in Seasonal Frozen Regions

Leilei Han [1], Haibin Wei [1] and Fuyu Wang [1,] *

[1] School of transportation, Jilin University, Changchun 130022, China; hanll18@mails.jlu.edu.cn(L.H.); weihb@jlu.edu.cn (H.W.)

* Correspondence: wfy@jlu.edu.cn; Tel.: +86-151-431-73491 (F.W.)

Abstract: Silty clay modified by fly ash and crumb rubber is a kind of sustainable subgrade filler which has good anti-freeze-thaw resistance stability but wake vibration isolation performance. The objective of this study was to improve the vibration isolation of the modified soil and investigate the vibration isolation effect of the composite subgrade structure of XPS plates and the modified soil by indoor impact test. First, the vibration isolation performance of silty clay, modified soil and composite subgrade structure was respectively evaluated. Second, the effect of XPS plate's thickness and vibration intensity on the vibration performance of the composite subgrade structure were evaluated. Third, the vibration isolation performance of the test groups under the condition of freeze-thaw cycles was assessed. The results show that the vibration isolation performance of subgrade can be effectively improved by setting XPS plates. The composite subgrade structure has certain vibration isolation effect, especially in vertical direction. Considering vibration isolation performance and costs, 5cm is the optimum XPS plates thickness. The composite subgrade structure has great vibration isolation performance under the condition of freeze-thaw cycles, so it is suitable to be applied in road subgrade in seasonal frozen regions.

Keywords: XPS plates; composite subgrade structure; vibration isolation; impact load test; freeze-thaw cycles

1. Introduction

The problem of environmental vibration caused by traffic load has attracted more and more attention with the rapid development of road traffic in recent years. Road traffic accounts for 11.3% of the total complaint rate of environmental vibration pollution and ranks third behind construction and factories according to relevant statistics. [1].

Vibration caused by traffic load may result in the strength decrease and the settlement increase of roadbed and foundation. The long-term vibration can cause serious damage to nearby buildings, threaten the comfortability of people's life and affect the normal use of precision instruments [2-3], which must be solved urgently. To solve the vibration pollution caused by trains, Costa [4] presented a model to understand the dynamic behavior of ballasted tracks with mats. It was found that the vibration could be reduced by placing the mat beneath the subballast. Bajcar [5] conducted the in-site experiments to measure the vibration levels of buried operating natural gas pipeline under the moving traffic. They focused on the assessment of the impact of the traffic-induced vibration and the increased risk on individuals which were affected by such underground natural gas pipeline at road crossing.

Based on the soil stabilization technology, a novel subgrade material that silty clay modified by fly ash and crumb rubber was proposed by our research group. It has been proved that the modified soil possesses greater performance in conventional physical properties, strength, deformation and stability, especially after freeze-thaw cycles [6-8]. This modified soil is also regarded as a sustainable subgrade material because it disposes and recycles the large amount of industry waste fly ash and

rubber products. The great resistance to freeze-thaw cycles contributes to the sustainable performance of the subgrade in seasonally frozen regions. However, many literatures show that the anti-vibration performance of soils modified by fly ash is poor, the liquefaction resistance decreases after multiple vibrations [9-10]. The research on anti-vibration of silty clay modified by fly ash and crumb rubber is scarce and worth studying.

The influence of vibration on sustainable performance of buildings can be effectively mitigated by the design and development of more efficient solutions. In road engineering, isolation layer is adopted against vibrations effectively. Expanded polystyrene foam sheet (EPS) is the most commonly used isolation material, which has the characteristics of ultra-light weight, good compressive property, high strength, good durability, thermal insulation [11-12]. Xiang [13] proved the significant vibration isolation effect of EPS on soils by the indoor model test. It was found that the closer EPS board and the vibration generator are, the better vibration isolation effect is. C.Murillo [14] studied the viability of EPS as the vibration isolation layer. The effect of barrier depth, thickness and distance from the vibration source on the vibration isolation of EPS was investigated.

XPS is a rigid foam board made of polystyrene resin, other raw materials and polymers, heated, mixed and injected with catalyst at the same time, and then extruded and molded. Compared with EPS, XPS (Extruded polystyrene) foam sheet has weaker hydroscopicity, lower thermal conductivity, higher compressive strength and more environmentally friendly characteristics [15,16]. It has been used as the functional layer (i.e. thermal insulation, vibration isolation and so on) beneath the building's foundation. Kilar et al. [17] performed the laboratory test to evaluate the performance of XPS board in earthquake engineering. They also revealed the failure mechanism of building structure founded by XPS board subjected to earthquake loading. Ozgur et al. [18] found that the presence of foam behind the flexible retaining wall could effectively result in a reduction of dynamic pressure and displacement. Mao et al. [19] summarized the achievements of protecting Qinghai-Tibet Plateau permafrost by XPS board. A series of valuable guidance regrading design, construction and quality control measures were given.

It's more valuable and promising to replace EPS with XPS board. However, the investigation into the application of EPS in practical engineering is much more than the corresponding research performed on XPS, especially in road engineering. In this study, XPS plates were adopted to improve the vibration isolation performance of silty clay modified by fly ash and crumb rubber. The composite subgrade structure of XPS plates and the modified soils was called the composite subgrade structure. The objective of this paper was to: (1) evaluate the vibration isolation effect of silty clay, the modified soil and the composite subgrade structure of modified soil with XPS plates; (2) determine the optimum thickness of XPS plates in the composite subgrade structure; (3) investigate the effect of vibration intensity and freeze-thaw cycles on the vibration isolation of the composite subgrade structure.

2. Materials and Methods

2.1 Materials

2.1.1 Raw materials

The soil used in this test was silty clay. Its physical properties were listed in Table 1. Fly ash was the silica alumina fly ash, which was provided by the Power Plant of Changchun. The content of SiO2+Al2O3 is 78.13~88.64%, CaO is 4.12~7.02%, SO3 is 0.1~0.72%, loss of ignition is 1.22~5.26%.

Table 1. Typical physical properties of silty clay.

Liquid limit	Plastic limit	Plasticity index	Optimum water content	Maximum dry density
34%	22.40%	11.60%	12.1%	1.92g/cm^3

The rubber particles were collected from Changchun Rubber Products Factory, whose grain size was 1 mm-1.5mm. They were recycled products of waste rubber tires.

XPS plates were made by Jilin Fuquan New Thermal Insulation Material Co., Ltd. The products had flat surface, no inclusions and uniform color. Its compressive strength was 256KPa.

2.1.2 Preparation of the modified soil

First, the raw silty clay and fly ash were dried, crushed and sieved through the seize of 2mm. Second, they were mixed at the dry mass ratio of 1:2. Then, rubber particles which accounted for 2% of the total mass were added. Finally, mix them evenly after the calculated amount of water was added into. According to the previous research of the research group [6-8], the modified soil in this mixture ratio has fairly good anti-freeze-thaw stability as a green and sustainable road subgrade material with good performance for seasonal frozen regions. Before testing, the mixture should be placed in the humidor for 24 hours. The physical indicators of the modified soil were listed in table 2.

Table 2. physical indicators of the modified soil.

Liquid limit	Plastic limit	Plasticity index	Optimum water content	Maximum dry density
36.0%	25.1%	10.9%	19.2%	1.61g/cm^3

2.2 Impact load test

2.2.1 Testing apparatus

The test model box (dimension of 0.3m×0.3m×0.5m) was made of iron plates (thickness of 3mm). Boundary reflection affects the test results seriously, especially in the case of small size and rigid boundary. To reduce this boundary reflection, XPS plates (thickness of 3cm) were placed at the bottom and surrounding of the model box, which was depicted in Figure 1. The small rigidity and high porosity of XPS could effectively reduce the boundary reflection.

Figure 1. Test model box

The piezoelectric acceleration sensor of DH311E and the acquisition instrument of DH5922 used in this study is made by Donghua Co., Ltd of China. To avoid being affected by moisture and soil when obtaining data, the acceleration sensor should be wrapped with waterproof plastic bags. The sensor and the acquisition instrument were illustrated in Figure 2.

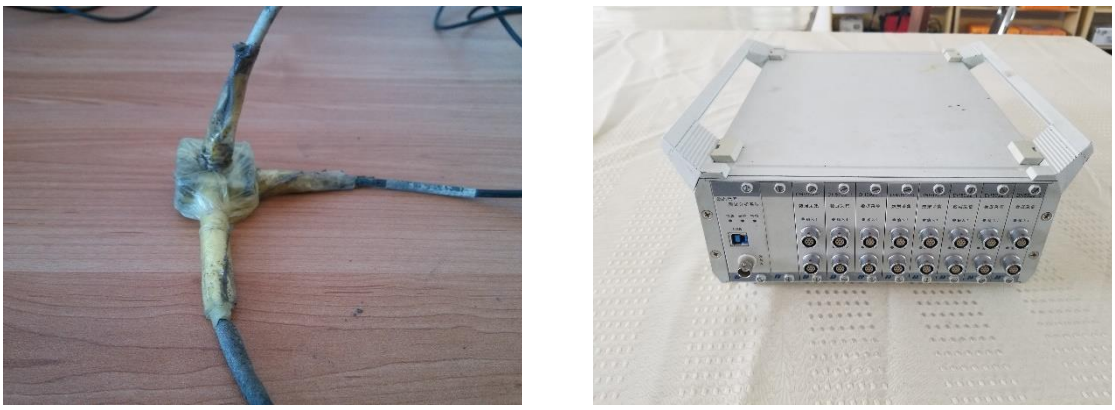

(**a**) (**b**)

Figure 2. Photos of sensor and acquisition instrument. (**a**) Acceleration sensor of DH311E; (**b**) Acquisition instrument of DH5922.

2.2.2 Impact load

The drop hammer was used to generate the vibration when applying impact load. The impact load applying device (which is listed in Figure 3) was composed by a drop hammer, a connecting bar and a round bottom plate (whose diameter is 9cm, thickness is 1cm).

Figure 3. Impact load applying device

Impact loads with different magnitudes could be achieved by adjusting the drop height of the hammer. The impact force can be calculated according to the law of conservation of momentum. It's considered that the plate provides the hammer a counter impulse with the equal value but opposite direction of the impact impulse. An acceleration sensor is placed on the bottom plate to calculate the counter impulse. Figure 4 is the diagram of collected acceleration versus time. The product value of the plate mass (m) and the area enclosed by acceleration curves with time (a*t) is equal to the value of counter impulse (F*t).

This counter impulse can be simulated by the triangular pulse shape [20,21], which is described as Figure 5. Just as shown, F_1 is the maximum point of the counterforce, T_1 are the interaction time. F_1 is regarded as the load force in analysis. In this study, the action time of the impact load is about 0.006s. Based on the collected data of load test, the impact load force and the corresponding stress of drop hammer falling from different heights are calculated, which is listed in Table 3.

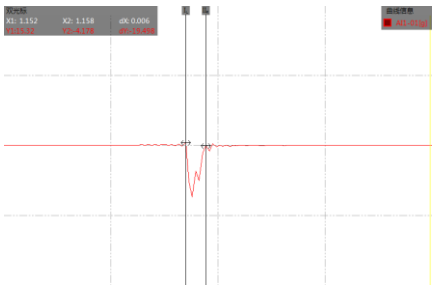

Figure 4. Diagram of collected acceleration versus time for impact load

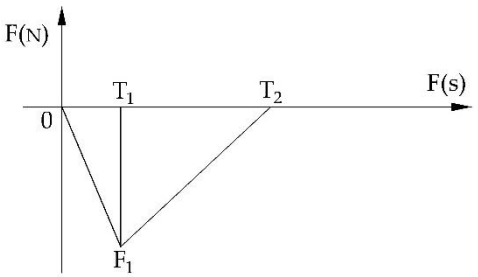

Figure 5. Equivalent triangular waveform of impact load

Table 3. The impact force and stress corresponding to the falling height.

	Drop height (cm)				
	5	**10**	**15**	**20**	**25**
Impact force (N)	100.78	142.52	174.55	201.55	225.34
Impact stress (Pa)	15845.91	22408.81	27444.97	31690.25	35430.82

2.2.3 Preparation of the test soils and sensors in mold box

According to the calculated compaction degree, the test soils were poured into the mold (by 5 layers, the thickness of each layer is 10cm) and compacted by hammer. In the process of compaction, acceleration sensors were buried at the designed depth. It should be paid attention to the accuracy of the location of sensors. Furthermore, to investigate the application viability of this composite subgrade structure in seasonally frozen areas, the vibration isolation test under freeze-thaw cycles was conducted. A temperature sensor was also buried in the mold to monitor the freeze-thaw cycles process.

2.2.4 Test procedures

Three test groups, respectively silty clay, the modified soil and the composite subgrade structure, were designed to study the vibration isolation effect. They are G (group) 1, G2 and G3, which were listed in Figure 6. For G1, the mold box was completely filled with silty clay. As for the other two groups, the upper 30cm of the soils were replaced by the modified soil and the composite subgrade structure, respectively. The sensor was buried at the depth of 30cm, which was exactly the bottom of the modified soils. In G3, different thicknesses (3cm, 5cm and 9cm) of XPS plates were used to determine the optimum thickness of the XPS plates. When testing, a slab of bitumen mixture (the size of 5cm×20cm×20cm) was placed at the top of test groups. The impact applying device was put on the surface of the asphalt mixture. The drop height of the hammer was set as 5cm, 10cm, 15cm, 20cm and 25cm to simulate the vibration waves of different intensities. As the drop hammer fell down, the vibration waves generated and propagated through the different layers. The fierce vibration and accelerations could be collected by the sensor. The vibration isolation effect of three test groups was assessed by a series of impact load tests.

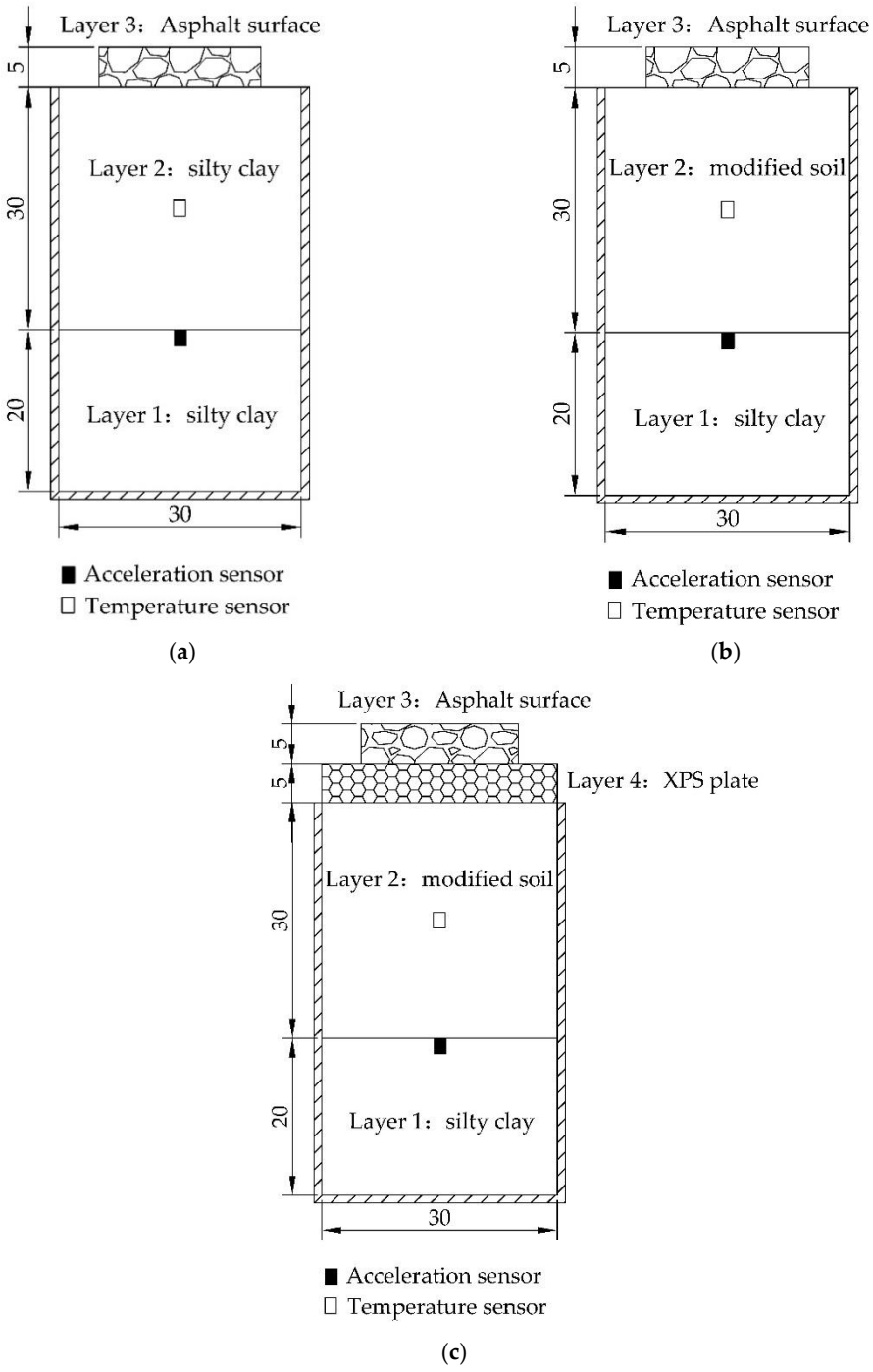

Figure 6. Diagram of sensors and filling materials of three test groups. (**a**) G1; (**b**) G2; (**c**) G3.

3. Results and Discussion

In this study, ten repeated operations for each test condition are designed. The transvers (X-direction and Y-direction) and the vertical (Z-direction) acceleration vibration waves are collected by the sensor, which are illustrated in Figure 7 as an example. The peak acceleration value of each wave is recorded, and the average value of ten acceleration peaks is calculated as the representative value to conduct the analysis of vibration isolation effect. The results of the indoor impact test under different test conditions (different thickness of XPS plates and different falling heights of drop hammer) are listed in Table 4, 5 and 6.

Preprints (www.preprints.org) | NOT PEER-REVIEWED | Posted: 29 April 2020 doi:10.20944/preprints202004.0508.v1

Peer-reviewed version available at Appl. Sci. 2020, 10, 3597; doi:10.3390/app10103597

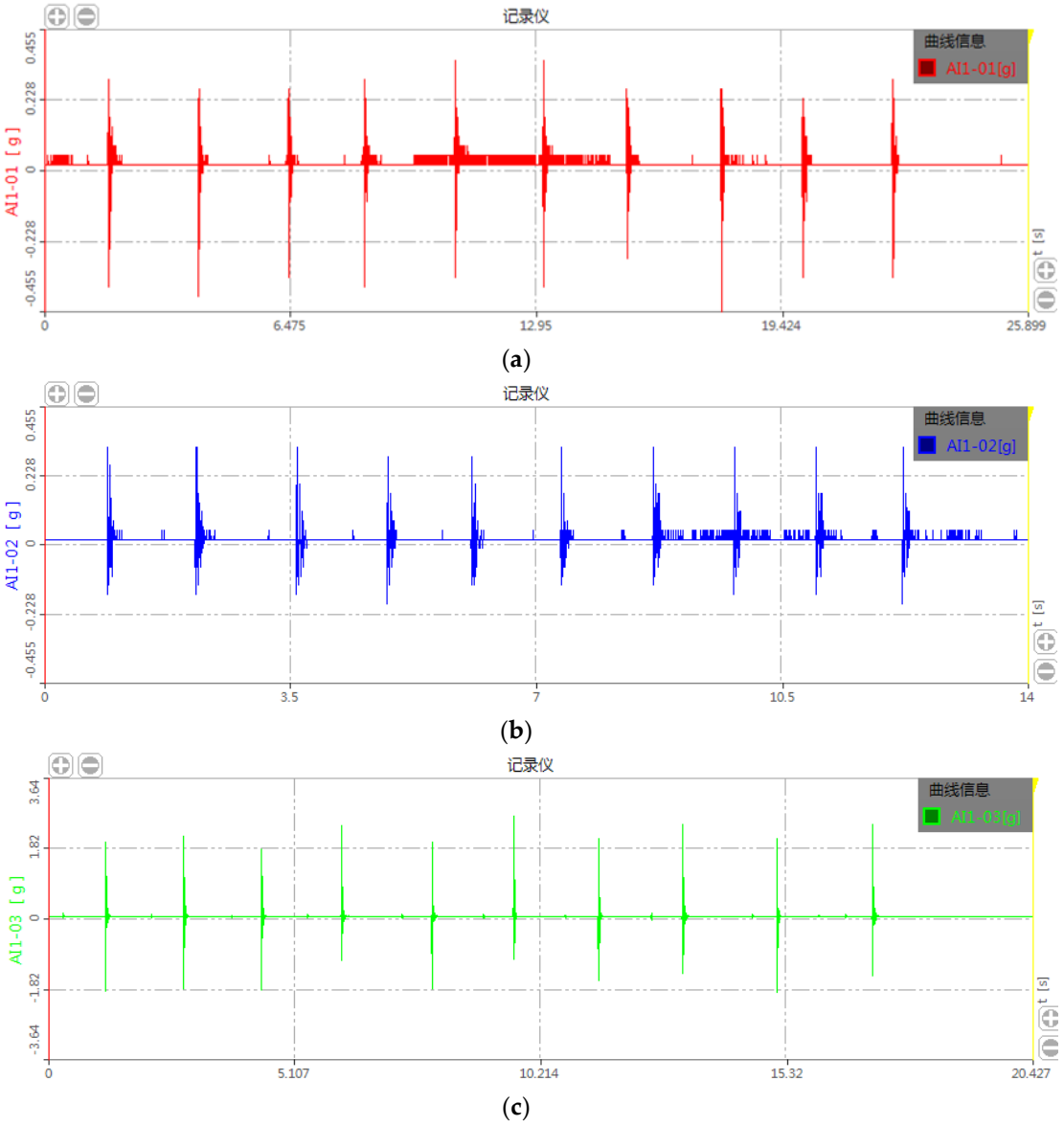

Figure 7. Measured acceleration wave curves. (**a**) Acceleration of X-direction; (**b**) Acceleration of Y-direction; (**c**) Acceleration of Z-direction.

Table 4. Peak value of X-direction acceleration.

Height of the fall	5cm	10cm	15cm	20cm	25cm
Modified soil	0.1818g	0.203g	0.2815g	0.336g	0.3903g
Silty clay	0.1908g	0.194g	0.233g	0.2875g	0.2756g
3cm XPS plate	0.0848g	0.1396g	0.1879g	0.2242g	0.2905g
5cm XPS plate	0.0819g	0.1213g	0.1427g	0.1907g	0.212g
9cm XPS plate	0.076g	0.088g	0.1335g	0.164g	0.176g

Table 5. Peak value of Y-direction acceleration.

Height of the fall	5cm	10cm	15cm	20cm	25cm
Modified soil	0.272g	0.2873g	0.2871g	0.3693g	0.4507g
Silty clay	0.1606g	0.2238g	0.2815g	0.2964g	0.3539g

3cm XPS plate	0.1481g	0.2422g	0.321g	0.354g	0.369g
5cm XPS plate	0.094g	0.1542g	0.251g	0.2752g	0.2968g
9cm XPS plate	0.082g	0.1546g	0.203g	0.257g	0.2814g

Table 6. Peak value of Z-direction acceleration.

Height of the fall	**5cm**	**10cm**	**15cm**	**20cm**	**25cm**
Modified soil	1.2744g	1.7267g	2.0253g	2.4321g	2.7335g
Silty clay	0.9825g	1.3739g	1.621g	1.8718g	2.1532g
3cm XPS plate	0.1565g	0.2819g	0.4096g	0.4894g	0.5692g
5cm XPS plate	0.0998g	0.1737g	0.2589g	0.2962g	0.3584g
9cm XPS plate	0.0767g	0.1027g	0.1253g	0.1647g	0.205g

3.1 The analysis on the vibration isolation effect of test groups

To compare the vibration isolation effect of silty clay, the modified soil and the composite subgrade structure, the relationship curves between the acceleration peak and falling heights of hammer for three groups are drawn, which is depicted in Figure 8.

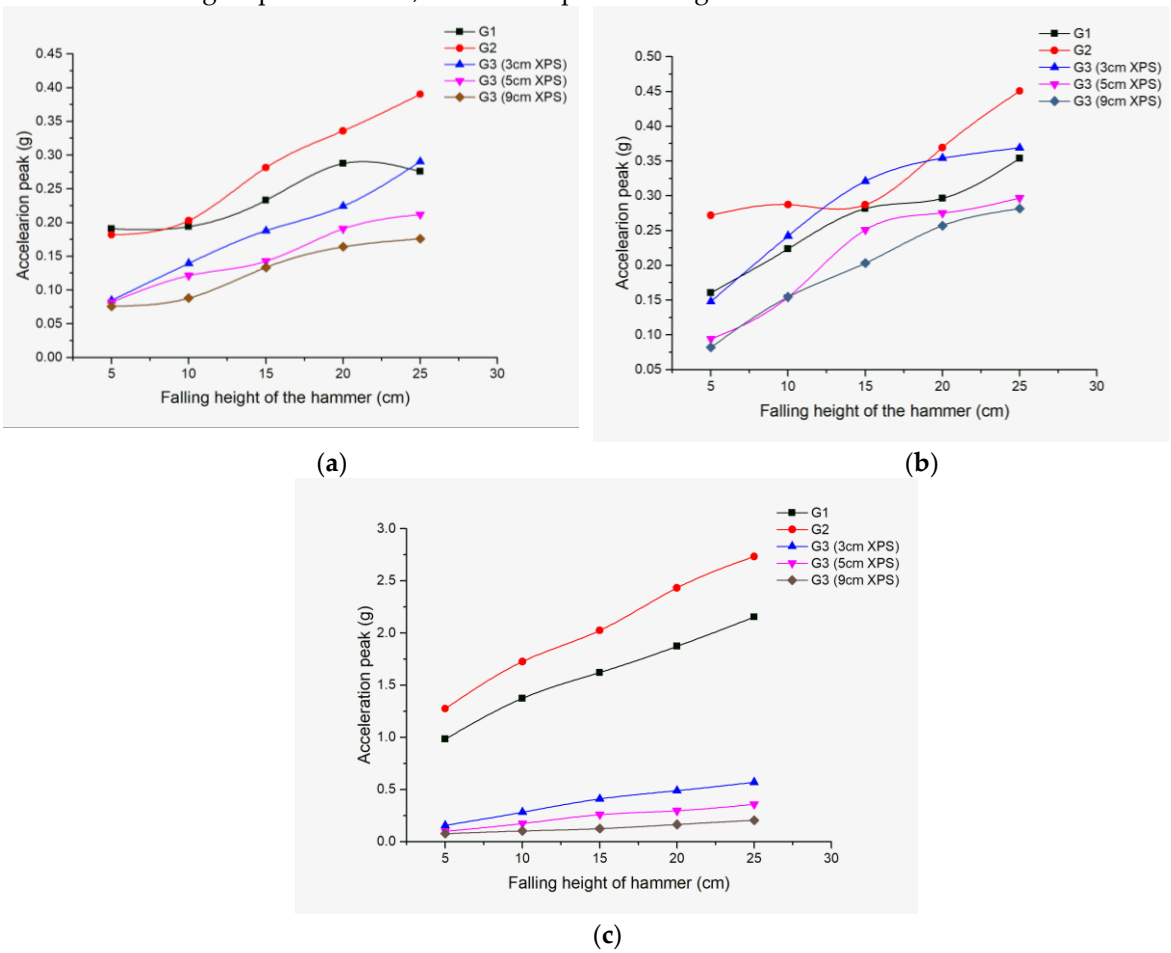

Figure 8. Acceleration peak values of three test groups. (**a**) Acceleration peak in X-direction; (**b**) Acceleration peak in Y-direction; (**c**) Acceleration peak in Z-direction.

From Figure 8, the acceleration peak values in three main axes (X, Y and Z-direction) for G1, G2 and G3 embedding different thickness of XPS plates raise as the falling heights increase. Comparing the data of G1 to G2, the acceleration peak values of G1 are lower than that of G2, especially in Z-

direction. It means the vibration isolation performance of the modified soil is worse than that of silty clay. The reason for this phenomenon is that fly ash reduces the damping of improved soil [22], while rubber particles increase the damping of modified soil. The strengthening effect of 2% rubber particles is very limited. The 32% content of fly ash dominates the change of damping of modified soil, which leads to the phenomenon that the damping of modified soil is less than that of silty clay and the vibration of modified soil is larger than that of silty clay. So, it's necessary to improve the vibration isolation performance of the modified soil subgrade.

Just as shown in Figure 8, the acceleration peak values of G3 are basically lower than that of G1, except the accelerations of G3 with XPS plates of 3 cm in X-direction and Y-direction. The results prove the viability of using XPS plates to improve the vibration isolation effect of the modified soil, especially using the thicker XPS plates. This phenomenon is attributed to the composition and structure of foam boards. Both EPS and XPS plates are made of polystyrene foam. The large amount of pores in the foam plate are beneficial to absorb the vibration and fluctuation [16,23]. The perfect closed-cell honeycomb structure makes the XPS plates have excellent stability, which is an important reason why it can be used as a light subgrade material.

Furthermore, it is noted that the acceleration peak values in Z-direction are far higher than that of X-direction and Y-direction. For road engineering, the vibration generated by traffic loads would propagate downwards the pavement structure. The vibration isolation effect in Z-direction is most concerned because the vibration in Z-direction is much larger than that in the other two directions, which has the greatest influence on the structure. The vertical vibration is considered as a vital parameter for measurement and construction control.

3.2 Influencing factors of vibration isolation effect for the composite subgrade structure

The previous section has proven the great vibration isolation of the composite subgrade structure. In order to investigate the vibration isolation effect of the composite subgrade structure with different thickness of XPS plates or vibration intensity (corresponds to different falling heights of hammer), the following analysis are conducted.

In this study, the isolation coefficient is adopted to evaluate the vibration isolation effect of the composite subgrade structure, which is defined as:

$$C=A_i/A_0 \quad (1)$$

where, C is the isolation coefficient, A_i is the acceleration peak value of the composite subgrade structure under different test conditions, A_0 is the acceleration peak value without setting the composite subgrade structure (corresponds to the acceleration value of G1). When $C < 1$, it means the vibration isolation effect is significant. The smaller the C value is, the better the vibration isolation effect is.

3.2.1 The effect of XPS plates thickness on the vibration isolation

Thickened XPS plates can effectively improve the vibration isolation performance of the composite subgrade structure. However, it sometimes causes the negative impact of overall structure and increases the usage cost. Therefore, it is vital to determine the optimum XPS plates thickness of the composite subgrade structure. In this part, the thicknesses of XPS plates are set as 3 cm, 5cm and 9cm respectively. The impact load is generated by hammer dropping from the height of 25 cm. The result is illustrated in Figure 9.

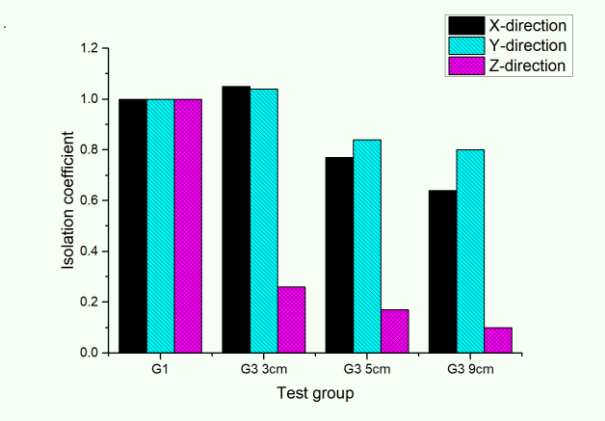

Figure 9. Isolation coefficient of the composite subgrade structure.

From Figure 9, the isolation coefficient of the composite subgrade structure decreases as the increase of the thickness of XPS plates. For G3, which embeds XPS plates with the thickness of 9cm, the isolation coefficient C in three main axes are 0.64, 0.80 and 0.10 respectively. The vibration isolation effect in Z-direction is obviously significant than that in the other two directions. It should be noted that the C value in X-direction and Y-direction for G3 embedding with 3cm XPS plates is greater than G1. It means the vibration isolation in transverse performs negative effect compared to G1. However, the vibration isolation effect in Z-direction of the composite subgrade structure is the most concerned problem. The relationship between isolation coefficient in Z-direction and the thickness of XPS plates is fitted in the exponential form, which is demonstrated in Figure 10.

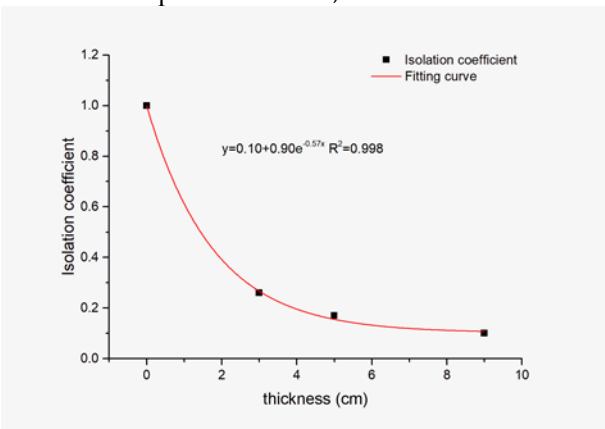

Figure 10. Fitting curve of isolation coefficient in Z-direction.

As shown in Figure 10, the XPS plates with the thickness of 5 cm and 9 cm both possess significant vibration isolation performance. The effect of the composite subgrade structure with 9 cm is slightly better. However, the enhancement in isolation performance is very limited when the thickness of the XPS plates increases from 5 cm to 9 cm. Besides, the cost of 9 cm XPS plates is much higher than that of 5 cm. So, the XPS plates thickness of 5 cm is considered as the optimum thickness of the composite subgrade structure in these test groups. The isolation coefficient C of the composite subgrade structure embedding 5 cm XPS plates in Z-direction is 0.17, which accords to the normal vibration isolation standard [24].

3.2.2 The effect of vibration intensity on the vibration isolation

In actual engineering, traffic loads with different weights always produce vibrations of different intensities. In this part, the vibration isolation performance of the composite subgrade structure subjected to different vibration intensities are investigated. The vibration of different intensities is achieved by load hammer falling from different heights (5, 10, 15, 20 and 25 cm). The thickness of XPS plates is 5 cm, which is determined in previous section. The results are shown in Figure 11.

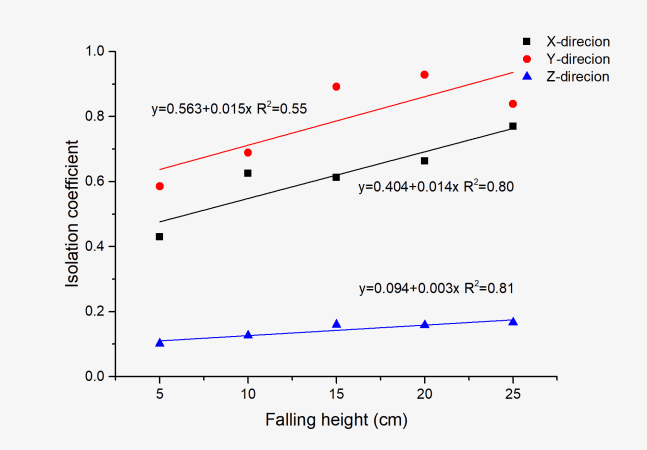

Figure 11. The isolation coefficient of the composite subgrade structure under different falling heights

Figure 11 shows that the isolation coefficient of the composite subgrade structure increases with the falling height increasing. To master the characteristics of isolation coefficient with the change of vibration intensity, the test data are fitted in linear forms, which are demonstrated in Figure 11. From Figure 11, it can be found that the correlation coefficients of X-direction and Y-direction are stronger than that of Z-direction. The slope value represents the decay rates of isolation coefficient with the increase of vibration intensity. The slope of X- direction, Y-direction and Z-direction are 0.014, 0.015 and 0.03, respectively. The decay rate of isolation coefficient in Z-direction is the lowest，which means the vibration isolation effect in the most concerned Z-direction has the smallest change with the increase of vibration intensity, showing good vibration isolation stability. Specifically, the vibration isolation coefficient increased by 62.7% (from 0.102 to 0.166) while the load intensity increased by 400% (from 5cm to 25cm). The vibration isolation effect of X-direction and Y-direction varies greatly with the increase of the vibration intensity. However, the vibration of X-direction and Y-direction is far less than that of Z-direction when the XPS plates is not set. In addition, the vibration isolation coefficients are all less than 1 in this study, which means that the vibration intensity of the XPS plates structure is less than that of the unset structure, so the vibration influence in X-direction and Y-direction is very limited. When the falling height of hammer is 25 cm, the isolation coefficient in Z-direction is 0.166, which is still lower than 0.2. So, it can be concluded that the composite subgrade structure possesses great vibration isolation performance in Z-direction even under great intensity vibration.

3.3 Vibration isolation of the composite subgrade structure after freeze-thaw cycles

The main reason of the road diseases in seasonally frozen areas is that the stability and durability of the subgrade material decrease after freeze-thaw cycles, which results in the increase of soil subsidence deformation and uneven sinking of road. It is necessary to ensure the anti-freeze-thaw performance of the composite subgrade structure in seasonally frozen areas. The acceleration peak value of the composite subgrade structure embedding 5 cm XPS plates after 1,2,3,4 and 5 freeze-thaw cycles are measured. The vibration isolation analyses in three main axes are conducted, as well as the comparative analysis with G1 and G2. The results are demonstrated in Figure 12.

Preprints (www.preprints.org) | NOT PEER-REVIEWED | Posted: 29 April 2020 doi:10.20944/preprints202004.0508.v1

Peer-reviewed version available at Appl. Sci. 2020, 10, 3597; doi:10.3390/app10103597

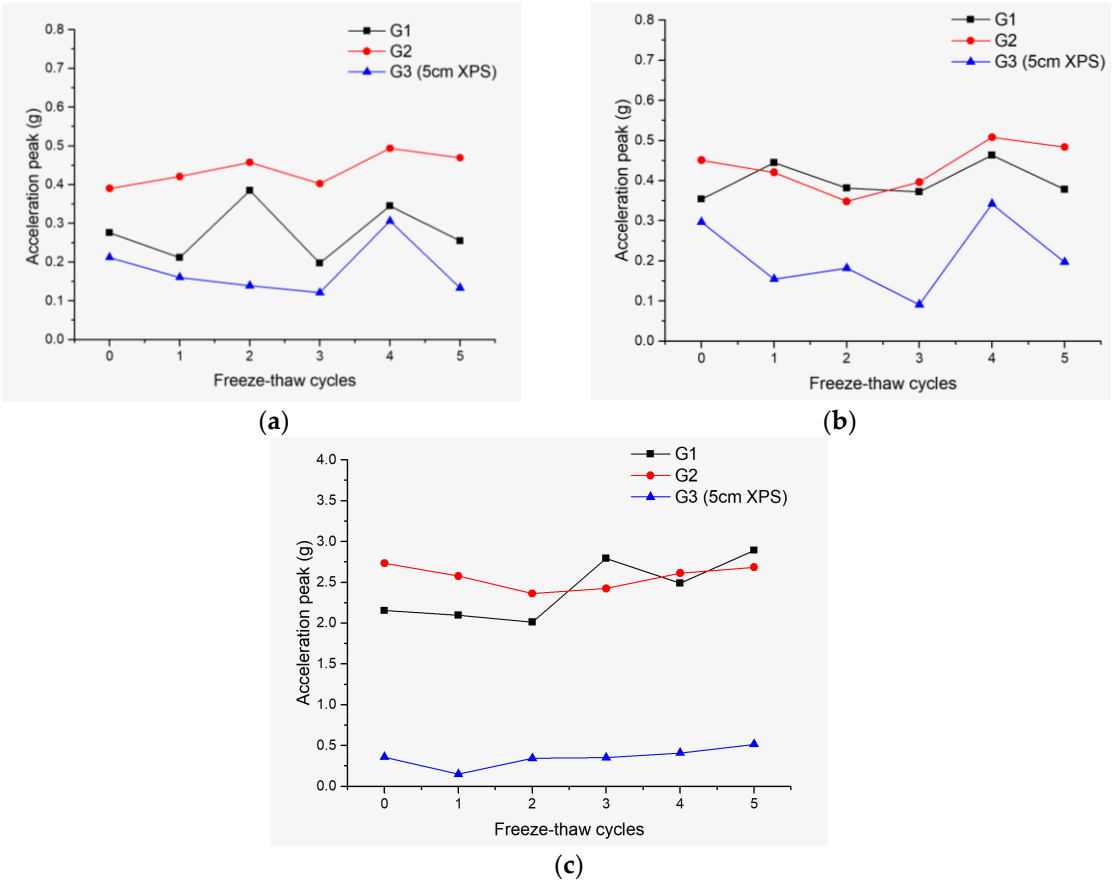

Figure 12. Acceleration peak of three test groups after freeze-thaw cycles. (**a**) Acceleration peak in X-direction; (**b**) Acceleration peak in Y-direction; (**c**) Acceleration peak in Z-direction.

From Figure 12, the acceleration peak values of three test groups fluctuate with the increase of freeze-thaw cycles, especially G1 (filled by silty clay). To better describe the fluctuation characteristic of acceleration peak, the statistical analysis is performed to calculate the mean, vibration range and standard deviation of G1, G2 and G3. The results are listed in Table 7.

Table 7. The static results of three test groups.

Direction	Type	Mean (g)	Range (g)	Standard deviation (g)
X-direction	G1	0.278	0.188	0.074
	G2	0.439	0.103	0.041
	G3 (5cm XPS)	0.179	0.185	0.070
Y-direction	G1	0.399	0.109	0.044
	G2	0.435	0.160	0.059
	G3 (5cm XPS)	0.211	0.251	0.093
Z-direction	G1	2.406	0.878	0.376
	G2	2.566	0.370	0.135
	G3 (5cm XPS)	0.355	0.364	0.139

Among three test groups, the mean values of G2 in three directions are all the largest, which means the vibration isolation of the modified soil is poor and the reason has been explained in 3.1. But the standard deviations and fluctuation ranges of G2 are small, which represents its stability of anti-freeze-thaw cycles is great. Comparing the results of G1 to G2, after 5 freeze-thaw cycles, the acceleration peak in Z-direction of G2 is close to that of G1. It means the vibration isolation performance of G2 is similar to G1 after 5 freeze-thaw cycles. However, the dynamic response stability of anti-freeze-thaw cycles for G2 is far better than that of G1. It indicates that the modified soil performed better than the silty clay when they go through the freeze-thaw cycles, that is the

reason why the modified soil is selected as a better subgrade filler in road engineering in seasonally frozen areas. The mean and range of G3 in Z-direction is the smallest. The mean value decreased by 86.2% (2.211g) compared with G2. The range and standard deviation are basically consistent with G2, decreasing by 1.6% (0.006g) and increasing by 2.9% (0.004g), respectively. These data fully prove the high efficiency and stability of vibration isolation effect of composite subgrade structure.

From above results, it can be concluded that the vibration isolation of the composite subgrade structure after several freeze-thaw cycles is still significant, especially in Z-direction. The isolation coefficients of the composite subgrade structure after freeze-thaw cycles are described in Figure 13. The isolation coefficients in X-direction and Y-direction fluctuate drastically. While the isolation coefficient in Z-direction maintains relatively stable. The isolation coefficients in Z-direction of the composite subgrade structure are all lower than 0.2, which reflects its great anti-freeze-thaw stability in terms of vibration isolation performance.

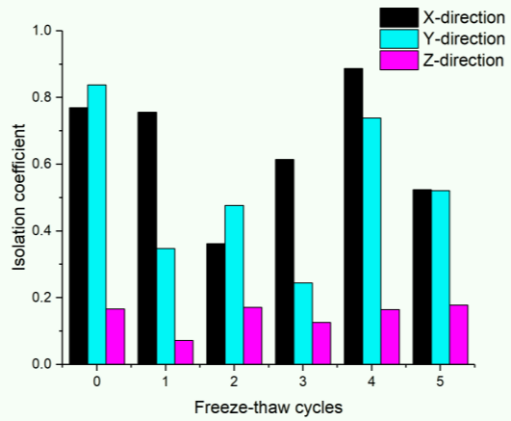

Figure 13. The isolation coefficient of the composite subgrade structure after freeze-thaw cycles.

4. Conclusions

In this study, XPS plates is adopted to improve the vibration isolation performance of the sustainable subgrade material (silty clay modified by fly ash and crumb rubber). The vibration isolation performance of the composite subgrade structure is evaluated by indoor impact test and numerical analysis. The conclusions are summarized as follows:

(1) The vibration of modified soil subgrade is greater than that of silty clay. The vibration of modified soil subgrade can be significantly reduced by setting XPS plates.

(2) Considering the effect and cost of vibration isolation, 5cm is considered to be the optimum thickness of XPS plates in road engineering.

(3) XPS plates has excellent vibration isolation stability under different vibration intensities. Laboratory test results show that the vibration isolation coefficient of subgrade model with XPS plates in Z-direction is less than 0.2.

(4) The vibration isolation performance of the composite subgrade structure has outstanding anti-freeze-thaw stability. The vibration isolation coefficient in Z-direction remains below 0.2 after several freeze-thaw cycles. This shows that the composite subgrade structure can be applied to the road engineering in seasonal frozen regions.

In summary, the vibration isolation effect of the composite subgrade structure is proven to be effective. For the modified soil (silty clay modified by fly ash and crumb rubber) subgrade, it will possess more sustainable vibration isolation performance by setting XPS plates. The indoor test results can provide a reference for design of the composite subgrade structure in practical application.

Author Contributions: Conceptualization, L.H. and H.W.; methodology, H.W.; software, L.H.; validation, L.H., H.W. and F.W.; formal analysis, L.H.; resources, F.W.; data curation, L.H.; writing—original draft preparation, L.H.; writing—review and editing, L.H. and F.W.; project administration, H.W.; funding acquisition, F.W. All authors have read and agreed to the published version of the manuscript.

Funding: This research was funded by the National Key R&D Program of China, grant number 2018YFB1600200; Science and Technology Project of Jilin Province Transportation Department, grant number 2017ZDGC6.

Acknowledgments: The authors express their appreciation for the financial support of the National Key R&D Program of China, grant number 2018YFB1600200; Science and Technology Project of Jilin Province Transportation Department, grant number 2017ZDGC6. Thanks to editors and reviewers for their efficient work.

Conflicts of Interest: The authors declare no conflict of interest.

References

1. Japanese Institute of Noise Control. *Regional Vibration of Environments*, Tokyo, Japan, 2001; pp. 8–9.
2. Qian, X.; Qu, W.; Li, Y.; Zhao, J. Vibration Isolation of Existing Buildings in Microvibration Traffic Environment. *Shock Vib.* **2019**, *2019*, 1-13. doi:10.1155/2019/1465638.
3. Watts, G.R.; Krylov, V.V. Ground-borne vibration generated by vehicles crossing road humps and speed control cushions. *Appl. Acoust.* **2000**, *59*, 221-236. doi:10.1016/S0003-682X(99)00026-2
4. Costa, P.A.; Calçada, R.; Cardoso, A.S. Ballast mats for the reduction of railway traffic vibrations. Numerical study. *Soil Dyn. Earthq. Eng.* **2012**, *42*, 137-150. doi:10.1016/j.soildyn.2012.06.014
5. Bajcar, T.; Cimerman, F.; Širok, B.; Ameršek, M. Impact assessment of traffic-induced vibration on natural gas transmission pipeline. *J. Loss Prev. Process Ind.* **2012**, *25*, 1055-1068. doi:10.1016/j.jlp.2012.07.021
6. Wei, H.; Jiao, Y.; Liu, H. Effect of freeze–thaw cycles on mechanical property of silty clay modified by fly ash and crumb rubber. *Cold Reg. Sci. Tech.* **2015**, *116*, 70-77. doi:10.1016/j.coldregions.2015.04.004
7. Li, C.; Liu, H.; Wei, H. An experimental study on engineering properties of rubber particles-improved fly ash soil. *Appl. Mech. Mater.* **2011**, *71-78*, 3401-3406. doi:10.4028/www.scientific.net/AMM.71-78.3401
8. Li, C.; Liu, H.; Wei, H. Experimental research on dynamic characteristics of fly ash soil improved by rubber particles. *Rock Soil Mech.* **2011**, *32*, 2025-2028+2033. doi:10.3969/j.issn.1000-7598.2011.07.018
9. Boominathan, A.; Hari, S. Liquefaction strength of fly ash reinforced with randomly distributed fibers. *Soil Dyn. Earthq. Eng*. **2002**, *22*, 1027-1033. doi:10.1016/S0267-7261(02)00127-6
10. Li, Y.; Chen, Y.; Li, M.; Peng, C. Dynamic characters laboratory test and the earthquake liquefaction characters of fly ash. *Journal of North China Institute of Water Conservancy & Hydroelectric Power*. **2002**, *23*, 64-67. doi:10.3969/j.issn.1002-5634.2002.04.020
11. Du, C.; Yang, J. Expanded Polystyrene (EPS) Geofoam: An analysis to characteristics and applications. *Journal of Southeast University (Natural Science Edition)*. **2001**, *03*, 138-142. doi:10.3321/j.issn:1001-0505.2001.03.032
12. Zhi, W.; Sheng, W.; Ma, W.; Qi, J. Evaluation of EPS application to embankment of Qinghai–Tibetan railway. *Cold Reg. Sci. Tech.* **2005**,*41*, 235-247. doi:10.1016/j.coldregions.2004.11.001
13. Xiang, G.; Ye, G.; Wang, J. Experimental investigation on propagation of impact load induced vibration in sandy soil. *Journal of Shanghai Jiaotong University*. **2012**, *46*, 136-141.
14. Murillo, C.; Thorel, L.; Caicedo, B. Ground vibration isolation with geofoam barriers: Centrifuge modeling. *Geotext. Geomembr.* **2009**, *27*, 423-434. doi:10.1016/j.geotexmem.2009.03.006
15. Gabriel, C. Gabriel Chemie introduces new flame retardant masterbatch for XPS boards. *Additives for polymers*.**2015**,*6*,3-4. doi:10.1016/S0306-3747(15)30066-X
16. Van Luck, F. Improving XPS insulation boards & new insulation products. *Cell Polym.* **2013**, *32*, 59.
17. Kilar, V.; Koren, D.; Bokan-Bosiljkov, V. Evaluation of the performance of extruded polystyrene boards – Implications for their application in earthquake engineering. *Polym. Test.* **2014**, *40*, 234-244. doi:10.1016/j.polymertesting.2014.09.013
18. Ertugrul, O.L.; Trandafir, A.C.; Ozkan, M.Y. Reduction of dynamic earth loads on flexible cantilever retaining walls by deformable geofoam panels. *Soil Dyn. Earthq. Eng.* **2017**, *92*,462-471. doi:10.1016/j.soildyn.2016.10.011
19. Mao, X.; Fan, K.; Yuan, K.; Li, J. Application of XPS plate as insulation layer in subgrade of highways in permafrost region. *Subgrade Engineering*. **2012**, *04*,15-19. doi:10.3969/j.issn.1003-8825.2012.04.005
20. Yu, Y. Study on dynamic response of frozen embankment under train vibration load. Master's thesis, Harbin Institute of Technology, Harbin, 2006.
21. Lin, J.; Deng, C.; Xu, J. Nonlinear dynamic buckling of FGM shallow conical shells under triangular pulse impact loads. *Advanced Materials Research*. **2012**, *460*, 119-126. doi:10.4028/www.scientific.net/AMR.460.119

22. Wang, J.; Wang, Q.; Wang, P.; Zhong, X.; Chai, S. Effect of adding amount of fly ash on dynamic constitutive relationship of modified loess. *Chinese Journal of Geotechnical Engineering*. **2013**,*35*,156-160.
23. Young, S. Experimental study on the thermal conductivity of thermal insulation materials used in residential buildings. *Advanced Materials Research*. **2014**, *1025-1026*, 535-538. doi:10.4028/www.scientific.net/AMR.1025-1026.535
24. Ministry of Ecology and Environment of the People's Republic of China. *Measurement method of environmental vibration of urban area (GB 10071-88).* China Communications Press: Beijing, China,1988. pp.1.